2025年臺灣國際科學展覽會 優勝作品專輯

作品編號 100049

參展科別 工程學

作品名稱 A Study on Hybrid Electromechanical

Actuators

得獎獎項 四等獎

就讀學校 International Computer High School of

Bucharest

作者姓名 Mendel-Emanuel Mendelsohn

Ioana Stanoiu

作者照片



A study on hybrid electromechanical actuators

1. Introduction

An actuator [7,22,28,29] is a motion control mechanism. Depending on the type of actuator, it can convert one type of energy (e.g. chemical, electromagnetic, thermal) into mechanical energy.

The field that laid the foundations for the realization of actuators is the field of electromechanics, whose evolution was common with that of actuators.

Thus, a periodization of the electromechanics paradigm includes 3 major stages [7,6,25,28,29]:

<u>I.1830-1950 Old electromechanics</u>. It is the period when the development of electric cars is significant, which imposed the appearance of classical or primary electromechanical drives.

It was a generous nineteenth century, dominated by the scientific results of the triumvirate: *Michel Faraday* (initiator of fundamental empirical experiments in the history of electricity; the law of induction, of the principle of electric motor, of the magnetic circuit, initiator of electro-chemistry), *James Clerk Maxwell*, (the genius theorist who put into mathematical form the equations of electric and magnetic fields, as well as the connection between them), and *Werner Siemens* (engineer and capitalist genius manager who managed to exploit and validate the relationship research-technology-economic development), triumvirate that can be disputed in the sense that other scientists also made outstanding contributions to the history of electricity: Edison, Ampere, Ohm (to name but a few who do not exhaust a significant list). Industrial production of electric machines also appeared and the first signs that will announce the emergence of electromechanical actuators as a basis for military applications.

<u>II.1950-1970</u>, <u>Traditional electromechanics</u>, in which electrical power drives appear, a theoretical and experimental development on the emergence of new material and electromechanical principles. Much military research (such as missile control or ship and torpedo control) influences and produces the transfer of applications in ordinary life, including the actuator subfield.

III. 1970-2020, Avant-garde electromechanics, representing according to Thomas Kuhn's theory, a paradigm forcing [30]. It is worth noting the contributions of the new scientific revolution.

- Specific technologies of miniaturization, by material deposition.
- Elastomeric polymeric materials with the help of which it was possible to make electrostrictive actuators,
- Very special means of investigation, mainly the development of microscopy,
- Gradient of applications in the field of medical engineering, with outstanding contributions both in investigation and microsurgery, applications of actuators in biological micropumps, etc. [25,27,28,29].

Electromechanical actuators are based on the conversion of a mechanical quantity (momentum, force, torque of forces) into electrical signals or vice versa. Any type of electric or magnetic field actuation obeys the laws of ponderomotor forces[5]:

For electric field:

$$\bar{f}_{el} = \rho_v \bar{E} - \frac{E^2}{2} grad\varepsilon + \frac{1}{2} grad\left(E^2 \frac{\partial \varepsilon}{\partial \tau} \tau\right)$$

And magnetic field, respectively:

$$\bar{f}_m = \bar{J} \times \bar{B} - \frac{1}{2}H^2 grad\mu + \frac{1}{2}grad(H^2 \frac{\partial \mu}{\partial \tau} \tau)$$

Where $\bar{f}=$ electric force density, respectively magnetic, $\rho_{v}=$ charge density, $\varepsilon=$ electrical permittivity of the medium, E= electric field strength, $\bar{J}=$ current density, $\mu=$ permeability of the medium, H,B= magnetic field intensity and induction, respectively, $\tau=$ mass density.

1.1Introduction to General Electromagnetic Field Laws and Theorems

The electromagnetic field is a classical field produced by moving electric charges. The electromagnetic field propagates in space at the speed of light and can interact with electric charges and currents. It can also be modeled as an overlap of an electric field with a magnetic field. Electric fields are produced by stationary electric charges and magnetic fields by moving charges (currents).

The electromagnetic field follows Maxwell's equations, namely:

- Gauss's law for the electric field $div \overline{D} = \rho$; D=electric field induction, ρ =free charge density;
- Gauss's law for the magnetic field

 $div \bar{B} = 0$; (no magnetic charges)

• Faraday's Law $curl \ \bar{E} = -\frac{\partial \bar{B}}{\partial t};$

• Maxwell-Ampere Law

$$curl \ \overline{H} = \overline{J} + \frac{\partial \overline{D}}{\partial t}; \qquad \overline{J} = \text{densitatea de curent},$$

 \overline{H} =intensitatea câmpului magnetic

For an electromagnetic wave propagating through a medium from Maxwell's laws can be deduced

$$div \, \overline{D} = 0$$

$$div \, \overline{B} = 0$$

$$curl \, \overline{E} = -\frac{\partial \overline{B}}{\partial t}$$

$$curl \, \overline{H} = \frac{\partial \overline{D}}{\partial t}$$

From which the speed of propagation of an electromagnetic wave through a homogeneous medium can be deduced:

$$v = \frac{1}{\sqrt{\mu \varepsilon}}$$

1. Initiation in the field of electromechanical actuators

From the theorems of ponderomotor actions, three independent electric and magnetic actuations can be distinguished, respectively:

 $\overline{f_{es}} = \rho_v \overline{E}$ - in the case of electrostatic type action that occur due to the interaction of charges with the electric field

$$\overline{f_{ep}} = -\frac{E^2}{2} grad\varepsilon$$
 -occurs in piezoelectric/anisotropic actuators; -if this type of actuation cannot exist $\varepsilon = constant \Rightarrow grad \varepsilon = 0$

 $\bar{f}_{els} = \frac{1}{2} grad \left(E^2 \frac{\partial \varepsilon}{\partial \tau} \tau \right)$ -electrostrictive type actuation occurs if the material has discontinuities, is composed of several media with different densities and permittivities

Analogously, we distinguish three magnetic-type forces

$$\overline{f}_L = \overline{J} \times \overline{B}$$
 –Lorentz force density

$$\overline{f_{m\mu}} = -\frac{1}{2}H^2grad\mu$$
 – magnetic force density that occurs when permeability depends on position

 $\overline{f_{mms}} = \frac{1}{2}H^2grad\left(H^2\frac{\partial\mu}{\partial\tau}\tau\right)$ - magnetostrictive force density that occurs when permeability varies with mass density

Each force describes an independent type of actuation. In the following we will study theoretically, and then experimentally, the possibilities of combining two types of actuation to obtain hybrid actuators with better performance.

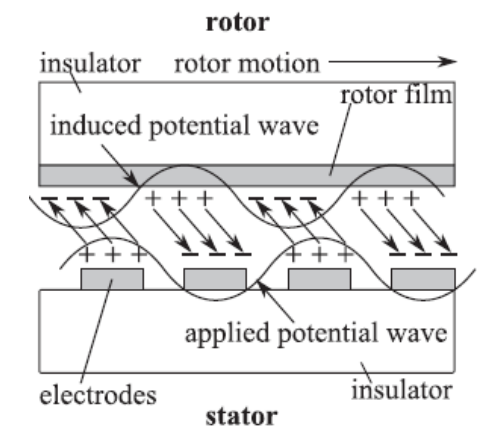
2. State of art - actuators and microelectronics

Miniaturization has been important for many technological advances that have taken place over the past 50 years. Since the invention of the integrated circuit in 1950, continuous improvements in microfabrication technology have allowed for an exponential decrease in the size of electronic components. The diversity, economy and power consumed by these electronic components have enabled the development of computers, digital cameras, mobile phones and other devices that have radically changed our world.

Micromotors

One of the major goals of research in the field is to create micro-robot machines that can perform different tasks in very small spaces. The researchers mainly explored motors based on electrostatic, magnetic and piezoelectric phenomena. Since research for silicon-based MEMS micromotors began in

the 1980s, a multitude of electrostatic micromotors have been tested. The first micromotors were those with variable capacity. An alternative to these motors, also developed in the 1980s, are electrostatic induction motors[8]. A simple model is the one in the figure in which the rotor is covered with a conductive layer and several electrodes are found on the stator. Applying a potential wave to the stator will form image charges on the roto and due to the attraction in them a torque acts on the rotor. One such 4mm diameter engine was built by a team of MIT researchers. The motor generated $3.5\mu Nm$ torque at speeds of 55000 cm and powered at 20mW



One such 4mm diameter engine was built by a team of MIT researchers. The motor generated 3.5 μ Nm of torque at speeds of 55000 rpm and powered at 20mW.

Motors based on electromagnetic forces are largely equivalent to electrostatic motors: variable magnetic reluctance motor is analogous to variable capacitance motor and magnetic induction motor is analogous to electrostatic induction motor. Just like electrostatic motors, they are also some of the first MEMS motors built and operational.

As for piezoelectric motors, most of them are designed to be used in resonance regime that is reached at high frequencies, therefore they are considered ultrasonic motors. Various models can generate torques ranging from a few nNm to mNm.

There are several known models for piezoelectric actuators, each with different applications: [31] Multilayered actuator: composed of approximately 100 piezoelectric blades separated from each other by electrodes. It has a small response time (10 μ s) and generates large forces (of the order of 1000N) for small voltages (100V), but the displacements are relatively small (10 μ m).

One of the industrial applications of this type of actuator is the print head of a matrix printer. This type of printer builds each character using a 24x24 array.

Bimorphic actuator - composed of multiple piezeoelectric and elastic plates and is built to generate large displacements of hundreds of microns, but the response time is longer than that of multilayered (~1ms) and much smaller forces (~1N)

Such a bimorph is used in the camera to close the shutter in just 1ms.

Currently, attempts are being made to expand the applications of piezoelectric actuators and improve actuation quality.

For example, materials that can withstand high temperatures are being studied. There is a high demand on the market for materials with piezoelectric properties that can withstand temperatures of hundreds of degrees Celsius. For this purpose, materials such as langasite (which does not undergo phase transformations except at temperatures above 1470 degrees Celsius) or gallium phosphate were tested.

Piezoelectric materials are increasingly used in the medical industry as well. Due to its ability to detect the human voice and respond to pressure waves, piezoelectric materials are being studied to create cochlear implants. These implants are used to remedy sensorineural hearing loss (a disease that occurs due to the inability of the inner ear to convert mechanical impulses coming from the eardrum into neural signals)

3. An analysis of theorems of ponderomotor actions in electrostatic field and magnetic field

According to the theorem of ponderomotive forces [5]:

$$\bar{f}_{el} = \rho_v \bar{E} - \frac{E^2}{2} grad\varepsilon + \frac{1}{2} grad\left(E^2 \frac{\partial \varepsilon}{\partial \tau} \tau\right)$$

$$\bar{f}_{m} = \bar{J} \times \bar{B} - \frac{1}{2}H^{2}grad\mu + \frac{1}{2}grad\left(H^{2}\frac{\partial\mu}{\partial\tau}\tau\right)$$

The possible types of actuation can be analyzed using 3 tables:

For electrostatic forces:

Table 1. Possibilities of combining electric field actuations

	$\overline{f_{e1}}$	$\overline{f_{e2}}$	$\overline{f_{e3}}$
$\overline{f_{e1}}$	X	$\overline{f_{e12}}$	$\overline{f_{e_{13}}}$
$\overline{f_{e2}}$	$\overline{f_{e21}}$	X	$\overline{f_{e23}}$
$\overline{f_{e3}}$	$\overline{f_{e31}}$	$\overline{f_{e32}}$	X

For magnetic forces:

Table 2. Possibilities of combining actuations in magnetic field

	$\overline{f_{m1}}$	$\overline{f_{m2}}$	$\overline{f_{m3}}$
$\overline{f_{m1}}$	X	$\overline{f_{m12}}$	$\overline{f_{m13}}$
$\overline{f_{m2}}$	$\overline{f_{m21}}$	X	$\overline{f_{m23}}$
$\overline{f_{m3}}$	$\overline{f_{m31}}$	$\overline{f_{m32}}$	Х

Electrical and magnetic forces can also be composed:

	$\overline{f_{m1}}$	$\overline{f_{m2}}$	$\overline{f_{m3}}$
$\overline{f_{e1}}$	$\overline{f_{em11}}$	$\overline{f_{em12}}$	$\overline{f_{em13}}$
$\overline{f_{e2}}$	$\overline{f_{em21}}$	$\overline{f_{em22}}$	$\overline{f_{em23}}$
$\overline{f_{e3}}$	$\overline{f_{em31}}$	$\overline{f_{em32}}$	$\overline{f_{em33}}$

Table 3. Possibilities of combining electric and magnetic field actuations

From each table we have the following possible combinations

-Table 1

$$\frac{\overline{f_{e12}}, \overline{f_{e13}f_{e23}}}{\overline{f_{e13}} = \overline{f_{e31}}; \overline{f_{e23}} = \overline{f_{e32}}; \overline{f_{e12}} = \overline{f_{e21}}; }$$

$$\frac{\overline{f_{e13}}, \overline{f_{e22}}, \overline{f_{e33}} - \text{cannot represent solutions}}{\overline{f_{e11}}, \overline{f_{e22}}, \overline{f_{e33}} - \text{cannot represent solutions}}$$

-Table 2

$$\frac{\overline{f_{m12}}, \overline{f_{m13}f_{m23}}}{\overline{f_{m13}} = \overline{f_{m31}}; \overline{f_{m23}} = \overline{f_{m32}}; \overline{f_{m12}} = \overline{f_{m21}}; \overline{f_{m11}}, \overline{f_{m22}}, \overline{f_{m33}}$$
- cannot represent solutions

-From Table 3, all forces are distinct. Some of this may not be practically feasible.

A separate analysis can be made for the third term of each force.

The third term of each force density being electrostrictive:

$$\overline{f_{els}} = \frac{1}{2} \operatorname{grad} \left(E^2 \frac{\partial \varepsilon}{\partial \tau} \tau \right)$$

and magnetostrictive, respectively:

$$\overline{f_{mms}} = \frac{1}{2} \operatorname{grad} \left(H^2 \frac{\partial \mu}{\partial \tau} \tau \right)$$

Through the development of terms, the following formulas are obtained:

$$\overline{f_{els}} = \frac{1}{2} \left(2 \frac{\partial \varepsilon}{\partial \tau} \tau \ grad \ E + E^2 \tau \ grad \ \frac{\partial \varepsilon}{\partial \tau} + E^2 \frac{\partial \varepsilon}{\partial \tau} \ grad \ \tau \right)$$

$$\overline{f_{mms}} = \frac{1}{2} \left(2 \frac{\partial \mu}{\partial \tau} \tau \operatorname{grad} H + H^2 \tau \operatorname{grad} \frac{\partial \mu}{\partial \tau} + H^2 \frac{\partial \mu}{\partial \tau} \operatorname{grad} \tau \right)$$

In the case of a dielectric material with constant permittivity (there can only be electrostatic actuations, i.e.: $grad\ \varepsilon=0; \frac{\partial \varepsilon}{\partial \tau}=0)\bar{f}_{el}=\rho_v\bar{E}$

But in the case of dielectric materials in which domains with different mass densities occur and permittivities vary with density (electrostrictive and piezoelectric forces occur. $\frac{\partial \varepsilon}{\partial \tau} \neq 0$)

In the case of a dielectric showing a continuous variation in permittivity with force density it can be written as:

$$\bar{f}_{el} = -\frac{E^2}{2}grad\varepsilon + \frac{1}{2}\frac{\partial\varepsilon}{\partial\tau}grad(E^2\tau); \quad \frac{\partial\varepsilon}{\partial\tau} = constant$$

(formula is valid if there is no distribution of free charges in the dielectric)

Analogous to ferromagnetic materials whose magnetisation strongly depends on the applied magnetic field:

$$\bar{f}_m = -\frac{1}{2}H^2grad\mu + \frac{1}{2}\frac{\partial\mu}{\partial\tau}grad(H^2\tau); \quad \frac{\partial\mu}{\partial\tau} = constant$$

(formula valid for case there are no currents through the material)

4. Experimental study of standard electromechanical actuators

4.1. Electrostatic actuators

These actuators operate on the basis of the theorems of electrostatics and material laws stated above. The computational relationships of electrostatic forces are included in the framework of ponderomotor force theorems. The first definition relationship, according to the theorem of generalized forces at constant load:

$$X_h = -\frac{\partial W_e}{\partial x_{q=ct}}$$

The electrostatic energy of a system of charges in a conductor is defined by the relation

$$W_e = \frac{1}{2} \sum_{j=1}^{n} q_j V_j$$

For linear environments where the relationship is valid $\vec{D} = \varepsilon \vec{E}$

$$W_e = \int w_e dv$$

Where is the volume density of electrostatic energy $w_e = \frac{1}{2} \varepsilon E^2$

For nonlinear environments where the integral is made on the volume bounded by the surface $W_e = \frac{1}{2} \oint V \vec{D} \vec{n} dA + \frac{1}{2} \iiint \vec{E} \vec{D} dv$.

In the case of a wave capacitor at the plane capacitor $W_e = \frac{1}{2}CU^2C = \frac{\varepsilon S}{g}$, S-active surface of the capacitor and g-distance between plates. Calculating the derivative can obtain the force of attraction between the plates, which can have different expressions depending on the shape of the capacitor and depends on whether it is powered at constant voltage (load varies) or is not powered at all (in which case the load on the armatures is kept constant and the voltage varies). An advantage of electrostatic actuators is that they can be made of lightweight materials (aluminum, silicone layers), they are useful in applications where mass is an important criterion. An example of an electrostatic actuator is even a capacitor with a dielectric. The energy of the capacitor without a dielectric is less than the energy of the capacitor with air between the armatures, so a force will be exerted on the dielectric that tends to pull it out between the armatures. Such actuators are used in microrobotics and microdrives for micromovements [7,8]. The disadvantages of electrostatic actuators is mainly that they require relatively high voltages (mostly in the range of 50-500V) and due to their small size it is possible to pierce the dielectric. Another impediment is friction that occurs between the mechanical components of the actuator (in bearings in the case of a rotor or or between dielectric and electrodes in the case described above)

4.2.Piezoelectric actuators

The piezoelectric effect is the property of some material to generate electric charges in response to the application of mechanical stress. One of the most important characteristics of the piezoelectric effect is reversibility: it exhibits both a direct and reverse effect. The direct effect occurs when, due to the deformation of the crystal under the action of an external force, the dielectric polarizes, and the reverse effect when, by polarizing the dielectric with an external source, a deformation of the crystal is obtained. The dielectrics used in the design of piezoelectric actuators are largely anisotropic and non-linear. In anisotropic materials electric field, induction, and polarization vectors are not collinear; They form a triangle.

We will discuss the relationships between field and induction in an anisotropic medium[6,7].

For any dielectric, the relationship between induction, field and polarization applies:

$$\overline{D} = \varepsilon_0 \overline{E} + \overline{P}$$

In the case of materials with anisotropes, the induction D is not parallel to the field. The equations between induction and field become:

$$D_{1} = \varepsilon_{11}E_{1} + \varepsilon_{12}E_{2} + \varepsilon_{13}E_{3}$$

$$D_{2} = \varepsilon_{21}E_{1} + \varepsilon_{22}E_{2} + \varepsilon_{23}E_{3}$$

$$D_{3} = \varepsilon_{31}E_{1} + \varepsilon_{32}E_{2} + \varepsilon_{33}E_{3}$$

From the law of energy variation it can be deduced that $\varepsilon_{ij} = \varepsilon_{ji}$

We can deduce a priority direction for which it is valid that induction is parallel to the field: $\bar{D} = \varepsilon \bar{E}$

Substitution yields the system of equations:

$$(\varepsilon_{11} - \varepsilon)E_1 + \varepsilon_{12}E_2 + \varepsilon_{13}E_3 = 0$$

$$\varepsilon_{21}E_1 + (\varepsilon_{22} - \varepsilon)E_2 + \varepsilon_{23}E_3 = 0$$

$$\varepsilon_{31}E_1 + \varepsilon_{32}E_2 + (\varepsilon_{33} - \varepsilon)E_3 = 0$$

For the system to have non-null solutions is for the determinant to be null

$$\Delta = \begin{vmatrix} (\varepsilon_{11} - \varepsilon) & \varepsilon_{12} & \varepsilon_{13} \\ \varepsilon_{21} & (\varepsilon_{22} - \varepsilon) & \varepsilon_{23} \\ \varepsilon_{31} & \varepsilon_{32} & (\varepsilon_{33} - \varepsilon) \end{vmatrix} = 0$$

From this we can solve an equation of degree 3 for priority permittivity from which the components of the priority/particular field can also be deduced.

For a piezoelectric blade, certain material coefficients are defined:

-modulus of elasticity at constant tension

$$c = g \left(\frac{\partial T}{\partial g}\right)_{II}$$
; T = unit effort and g = blade thickness

-dielectric permittivity of the blade at constant thickness

$$\varepsilon = \frac{g}{S} \left(\frac{\partial q}{\partial U} \right)_g$$

-piezoelectric coefficient at constant effort

$$d = \left(\frac{\partial g}{\partial U}\right)_T$$

-piezoelectric coefficient at constant load

$$h = -\left(\frac{\partial U}{\partial g}\right)_q$$

With the help of these coefficients and the relationships between mechanical parametric (stress and deformation) and electrical ones (field and induction) 8 equations specific to the piezoelectric effect can be written

For mechanical quantities (e-deformation and T-effort)

$$e = (s)^E T + dE (1)$$

$$e = (s)^D T + gD \quad (1')$$

$$T = (c)^E e - k_p E \quad (2)$$

$$T = (c)^D e - hE \quad (2')$$

For electrical sizes

$$(3)D = (\varepsilon)^T E + dT$$

$$D = (\varepsilon)^e E + k_p e \ (3')$$

$$E = (\beta)^T D - gT \ (4)$$

$$E = (\beta)^e D - he \quad (4')$$

Where Lorentz's coupling factor is called, s is elastic compliance or susceptibility, and is another material constant. $\beta k_p = cd = \varepsilon h$

In the case of the reverse effect, voltages in the range 0-50V were applied and the displacements were measured using an interferometer with nanometer precision (details about the measuring unit in *Annex* 1). The results were shown in the graph in Fig. 3:

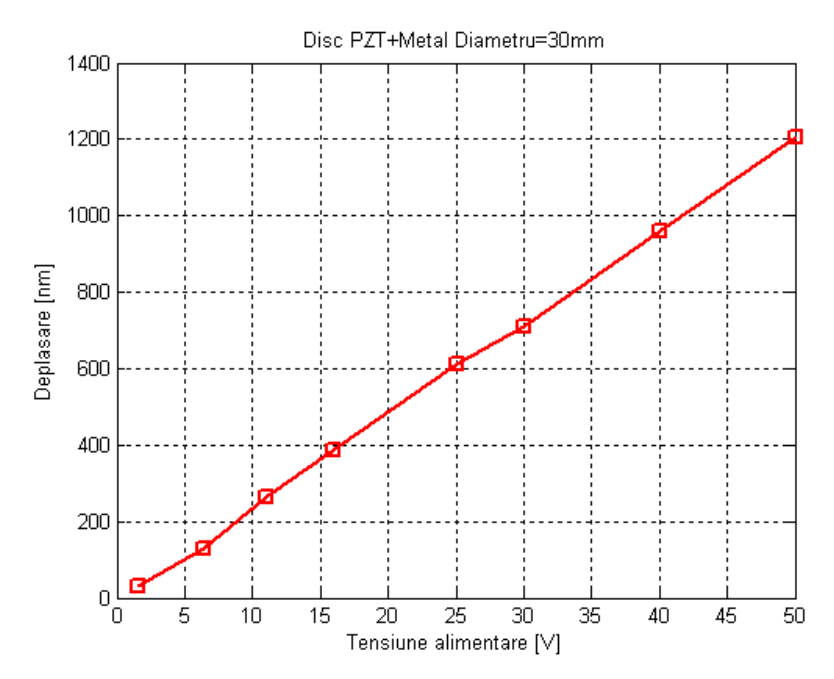


Fig 3. The displacement-voltage characteristic of the PZT piezoelectric actuator. The red line joins points whose coordinates have been measured experimentally

The thickness of the disc used is 0.5mm. From the graph we can observe an approximately linear dependence of the displacement depending on the applied voltage. This linear feature shows us that the drive is simple and precise. An important observation is that a deformation of 1 micron is obtained at about 42 V. So at 420 volts a deformation of 2% is obtained.

Piezoelectic actuators also have certain disadvantages, namely they are very sensitive and can lose their properties if they are applied too high forces or kept in humid conditions. Also, piezoceramic material (PZT) have quite low Curie temperature (~ 350 degrees Celsius) that do not allow them to operate in high temperature conditions (above 250 degrees Celsius they begin to lose their ferroelectric properties becoming paraelectric)

4.3 Unconventional actuators based on collagen and polymeric membranes.

In the following we will discuss the properties and actuation domains of certain collagen and elastomeric membranes in direct current.

Collagen is a multifunctional family of proteins with unique structural characteristics. It is the most common protein in the body, serving a multitude of biomechanical functions in bone, skin, tendons and ligaments. The simplest amino acid present in collagen is Glycine. Collagen is composed of three chained polypeptides, each with the general sequence of amino acids (Gli-Pro-Hip)n, glycine, proline, and hydroxyproline. Collagen has a triple helix structure in which the three left spiral polypeptide strands interact with each other "intertwining" around an imaginary axis, resulting in a common right spiral.

In experiments, 3 membranes (PE2, PE3, PE4) were tested and it was found that membranes with majority collagen content respond best.

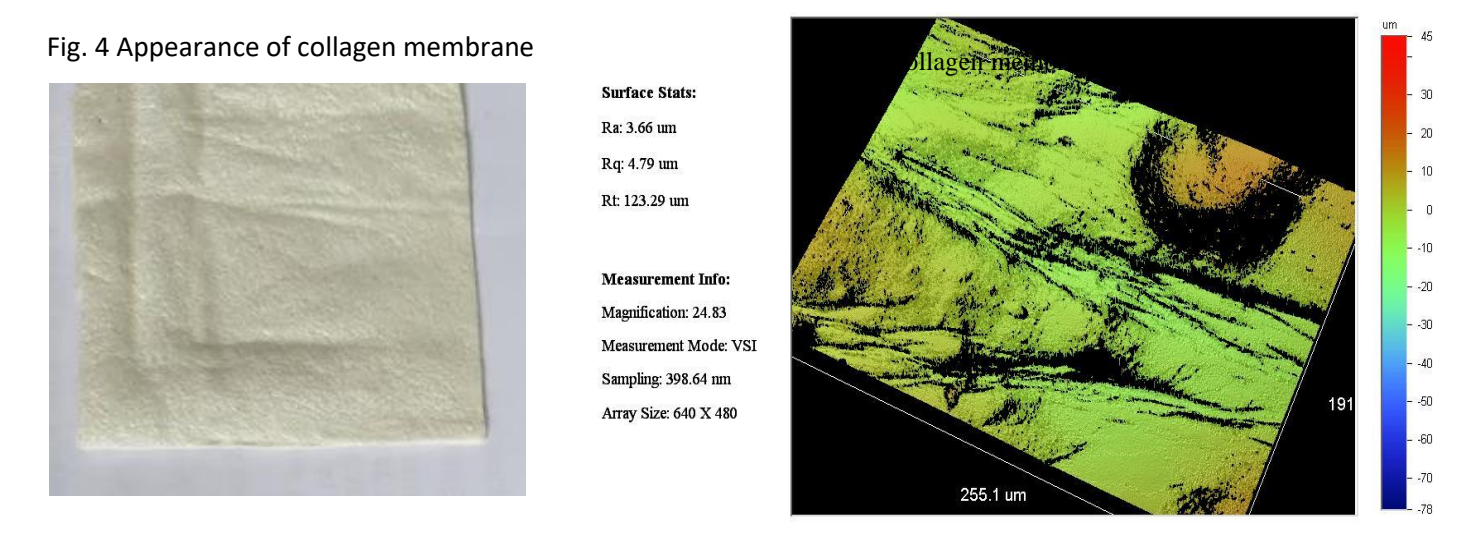


Fig.4 shows the appearance of the collagen membrane as seen at macroscopic level. In Fig.5 there is a profilogram of the membrane that highlights certain features of it at the microscopic level. The surface of collagen membranes is characterized by an average total roughness between $30 \div 50 \, \mu m$. Several areas with the area of $191 \, \mu m \times 255 \, \mu m$.

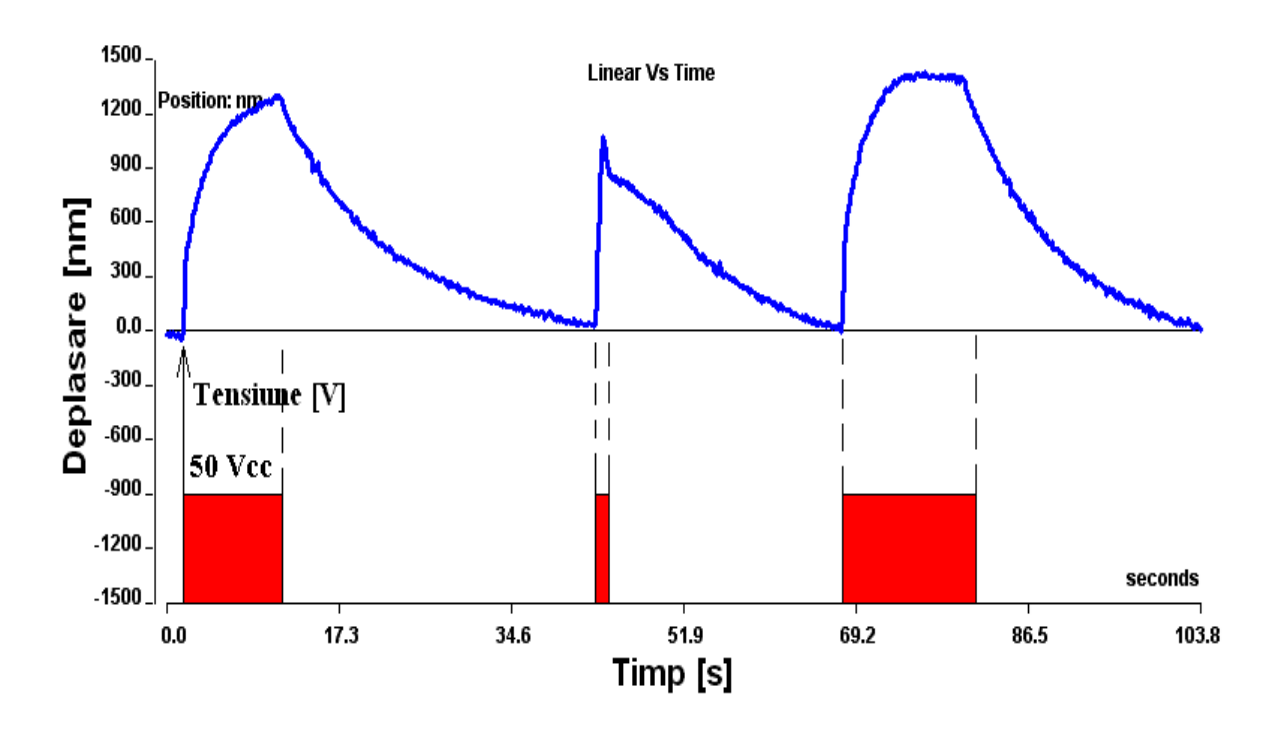


Fig. 6 Several PE3 membrane polarization-depolarization cycles

Fig. 6 shows several charge-discharge cycles for the PE3 collagen membrane at a voltage of DC 50V. The maximum displacement achieved is $1.4\mu m$. The PE3 membrane responded best to the tests, being the one that withstood the most high voltages, the others gradually losing certain properties.

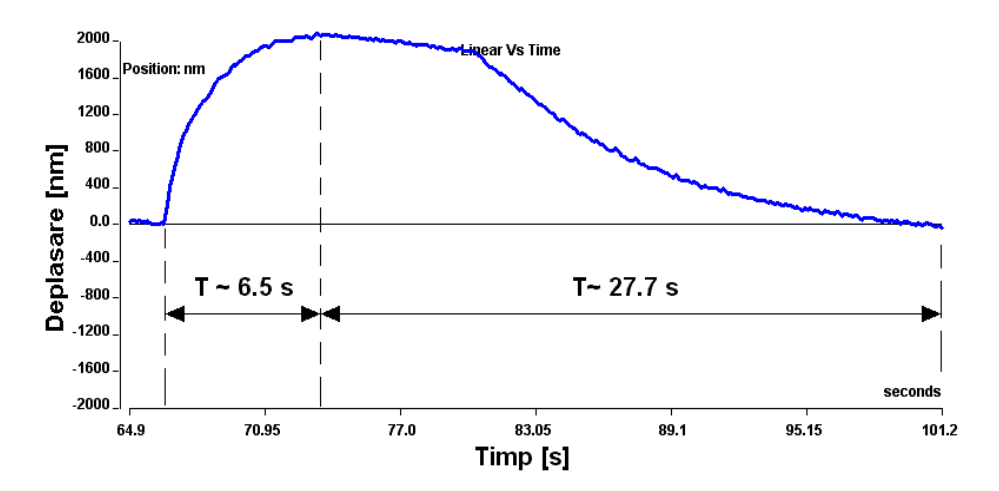


Fig.7 Single cycle of PE3 membrane

In Fig. 7, a polarization-depolarization cycle of the collagen membrane was analyzed in detail. Compared to a PZT material that depolarizes only by a forced discharge on a resistance or by short circuiting, charged collagen membranes depolarize themselves over time, regardless of the direction of the applied electric field.

Collagen membranes polarize slowly over time, charging time with electric charge is on the order of seconds, 6.5 s and discharge time is almost half a minute (~27.7s). Like any piezoelectric material, collagen is primarily a dielectric, implicitly the membrane is a capacitor with the capacitance between $200 \div 300~pF$, considering the area of the electrode $A = 0.00015~m^2$ and a thickness of the membrane $d = 0.17 \div 0.21~mm$. The calculated relative permittivity is $\varepsilon_r = 34 \div 42$.

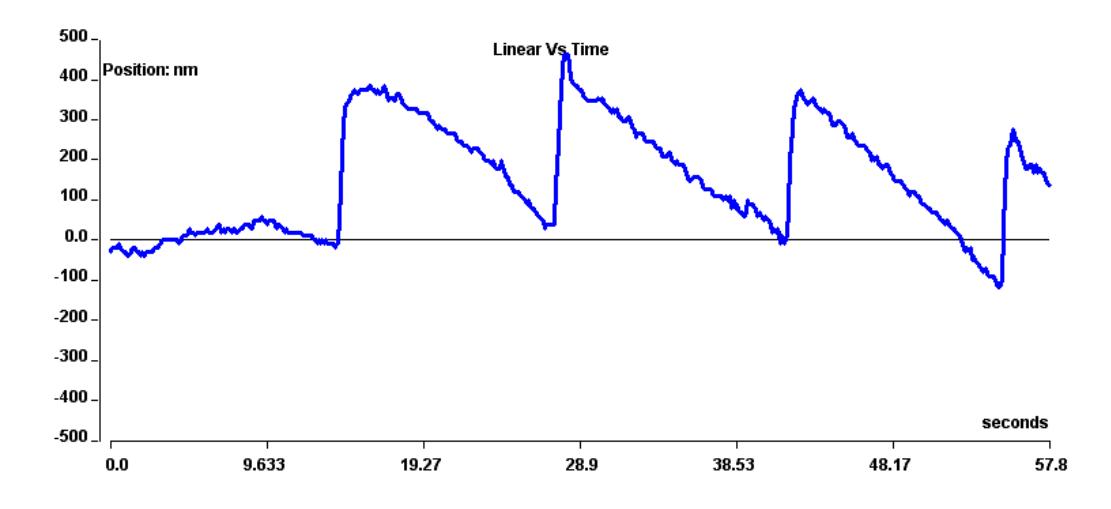


Fig.8 Several polarization-depolarization cycles for PE4 membrane

In Fig.8 are present the measurements on the PE4 membrane also in switching mode powered at 30V. It is observed that this membrane polarizes much faster than the other, and the depolarization is almost linear in time; The depolarization time is approximately 12.66s.

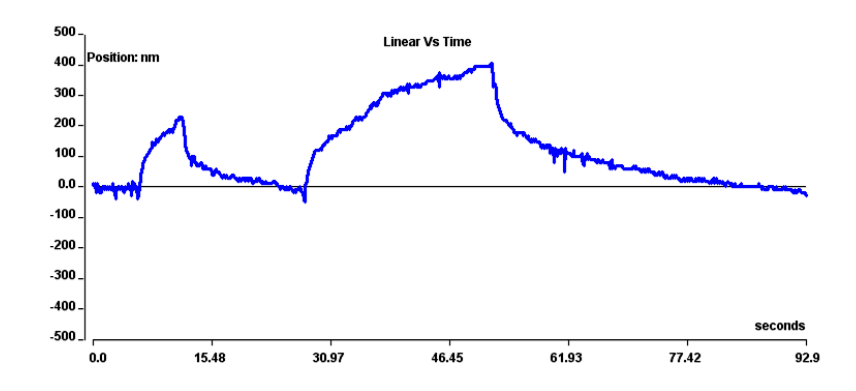


Fig.9 5H membrane powered at 10V DC, switching mode

The 5H membrane is a polymeric membrane doped with approximately 20% fine pyrite powder. Some of these pyrite-doped membranes have pierced at fairly low voltages due to breaches created by certain pyrite particles that can short-circuit the two power electrodes on either side of the sample.

The membrane shows a very good uniformity, in the distribution of pyrite particles no agglomerations of particles are observed, the polymer completely isolates these conductive particles.

The 5H membrane has been tested several times at lower voltages or up to 10 V direct current. It is remarkable that significant displacements of the order of 300-400 nm were achieved at a supply voltage of only 10 V. The membrane can compare or even exceed the performance of an ordinary piezoceramic material. The clamping force required to fix the membrane was 2.2 N, otherwise each of the membranes mentioned supports the weight of the retroreflector of 224 grams.

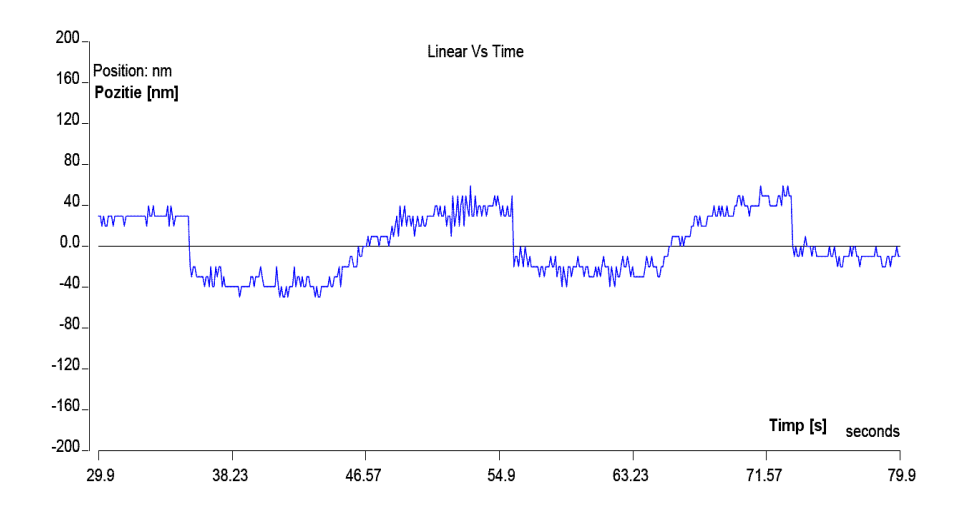


Fig.10 A quartz wafer powered at DC 475V, switching mode

The graph in Fig. 10 represents the time displacement dependence of a quartz plate switched to DC 475V.

The axis has not been adjusted to compensate for deformation caused by the retroreflector placed on the plate. Thus, the deformation is negative and reaches a value of about 80nm. The polarization time is almost negligible, but the discharge time has a value of about 7.2s. Quartz is widely used as a resonator at frequencies of 1-10 MHz to GHz.

It is also important to note that at small deformations the material generates very high voltages.

Elastomers

In order to study polymeric materials with elastomer basic structure, two types of inorganic silicon powders were prepared, differing in the inorganic component used.

A polymethylsiloxane with a molecular viscosity of approximately 400,000 and 6 % methylvinylsiloxane molar units were synthesized by cationic polymerisation of octamethylcyclotetrasiloxane in the presence of H2SO4 as catalyst. The reaction occurred at room temperature.

The resulting polymer was mixed with a solution of hydrophobic silicon dioxide as a hardening agent. 20% inorganic powder was introduced into the resulting HTV40 compound using a Yanke-Kunkel laboratory mixer equipped with Duplex vanes and a cooling jacket.

The resulting composites were cast into a metal frame and then pressed between two glass plates. This assembly was maintained for 2 hours at 150oC, during which time the maturation process of the composite element took place. The EH1 elastomer was prepared from the polymer matrix together with only the hardener to be able to judge the difference between the three different materials, depending on the application.

Code membranes	Composition
EH1	HTV40
EH5	HTV40, 20% MPQ ZS-9
EH6	HTV40, 20% pyrite

Table 4. Elastomeric membranes and their composition

The electrodes used in the following experiments are thin and elastic, made of copper foil about 0.1mm thick.

Fig. 11 shows the measurements made on the EH1 membrane in switching mode at DC 475V.

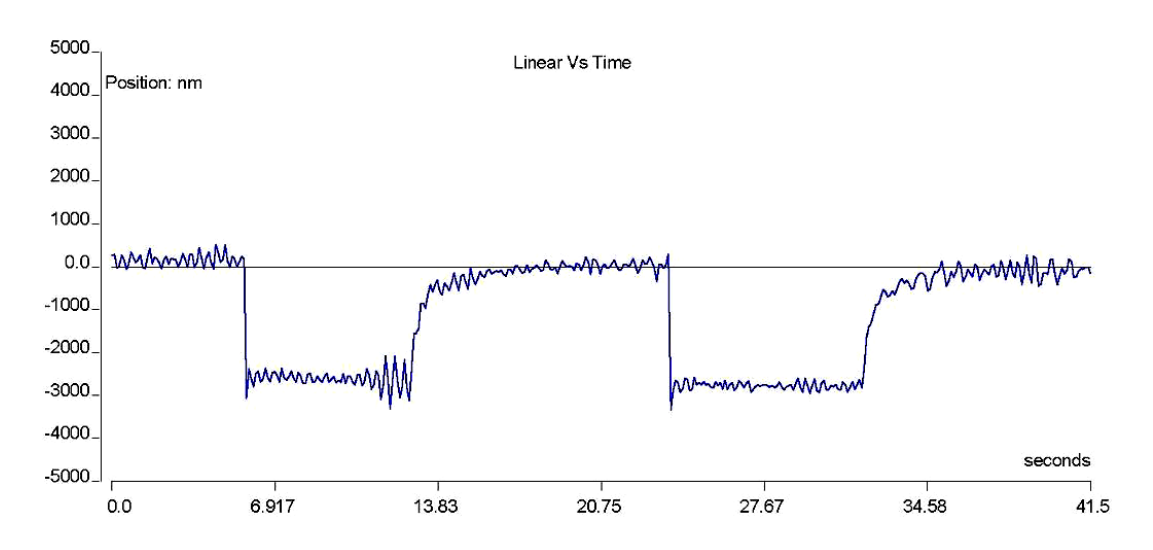


Fig.11 EH1 elastomer at DC 475V switching mode

The response time of the elastomer is negligible (polarization occurs almost instantaneously), whereas depolarization takes about 3.46s. It is also found that the displacement is negative and the maximum displacement (at equilibrium) is 2.7µm.

Slightly better results are obtained for the EH6 membrane which is similar to the one above, the difference being that it is doped with pyrite:

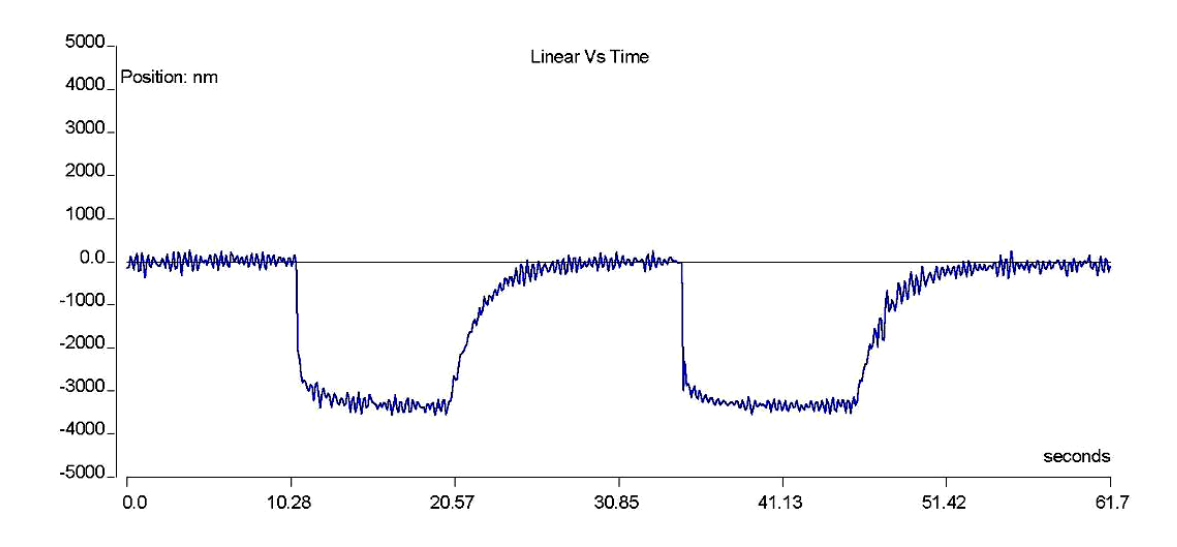


Fig.12 EH6 elastomer at DC 475V switching mode

It is observed that the displacement is still negative, but in the case of this mebrane the deformation when reaching equilibrium is $3.3\mu m$. Also, reaction times and return to baseline are longer (although 90% of total displacement is performed almost instantaneously), namely 3.43s and 6.36s, respectively.

For this study we will use only the dependencies of material displacements on applied stresses.

The other measured parameters may be relevant for integrating these actuators into various systems depending on the performance required (if a rapidly polarizing/depolarizing material, etc.) is required. The results of the above measurements, as well as other measurements, have been summarised in the table below

Membrane	Collagen PE4	Collagen PE3	Elastomer EH1 (HTV40)	Elastomer EH6 (HTV40+20% pyrite)	5H polymer with 20% pyrite	Polyimide with 10% BaO+TiO2	Quartz with 9% Ge
Voltage (V)	30	50	475	475	10	66	480
Displacement (µm)	0.5	1.4	2.7	3.3	0.4	0.07	0.08

Table 5. Measurement results (displacement and voltage) for the membranes studied

The best displacement/voltage ratio is obtained for polymer with 20% pyrite, but this material can only be used for low voltage applications because the breakthrough voltage is low.

Collagen membranes also give promising results and can perform almost as well as PZT material.

Quartz has applications in devices involving the direct piezoelectric effect, as it can generate high voltages for small displacements.

Elastomers have the fastes and most precise response out of the materials tested. Due to their abbility to deformate only slightly at low voltages, these membranes may be used to construct a piezoelectric-elastomeric actuator. This actuator would have a large actuation domain, being able to controll displacements on a large scale with high precision set by the elastomeric element.

4.4 Electromagnetic and electrodynamic actuators

A simple type of electrodynamic actuator can be the one in Fig.13 which consists of two long wires powered by alternating current.

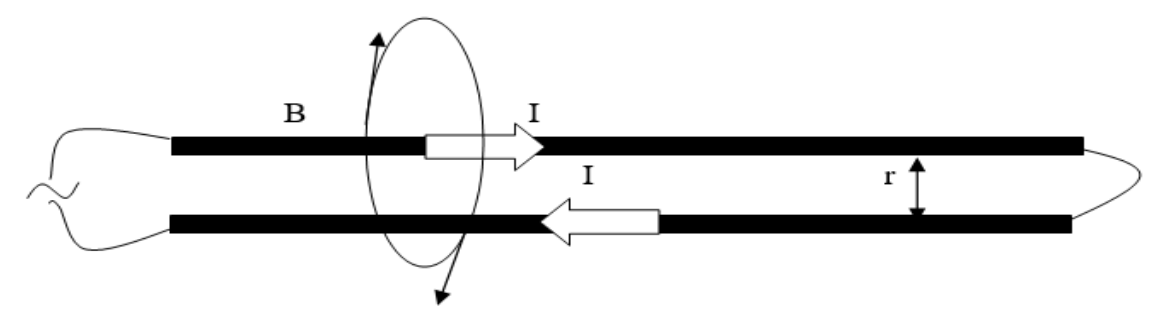


Fig. 13 An electrodynamic actuator consisting of two conductive wires

The magnetic field given by one of the remote cables r can be calculated using Ampere's law:

$$B * 2\pi r = \mu_0 I;$$
 $B = \frac{\mu_0 I}{2\pi r}$

Force on a conductor through which current passes in magnetic field:

$$F = BIL = \frac{\mu_0 I^2}{2\pi r} L$$

In our case, the current flows in the opposite direction in the two cables, so the force will be attractive. Applying an alternating current, the two wires will begin to vibrate, driven by the force that radiates in proportion to the square of the current intensity. Such systems can generate strong vibrations.

Electromagnets

Today, many medical devices, such as those used in therapy or magnetic resonance imaging, use electromagnets that generate large magnetic fields mainly using coils, ferromagnetic cores and permanent magnets connected to each other in a magnetic circuit.

Between magnetic and electrical circuits the following analogues can be established:

The magnetomotive force is defined as the contour integral of magnetic field strength:

$$\mathcal{F} = \int \vec{H} \cdot \vec{dl} = NI$$

The last equality being the consequence of the Maxwell-Ampere law.

In electrical circuits, Ohm's law relates the electromotive voltage applied to an element to the current passing through it:

$$IJ = IR$$

Its equivalent in magnetic circuits is Hopkinson's law:

$$\mathcal{F} = \phi \mathcal{R}$$

Waves -magnetomotor force, -magnetic reluctance/resistance and -magnetic flux through the circuit. The law is used, analogous to Ohm's law, to find the magnetic resistance of a circuit. $\mathcal{FR}\phi$

The magnetic resistance can be defined depending on the permeability, length and transverse area of the element:

$$\mathcal{R} = \frac{l}{\mu A}$$

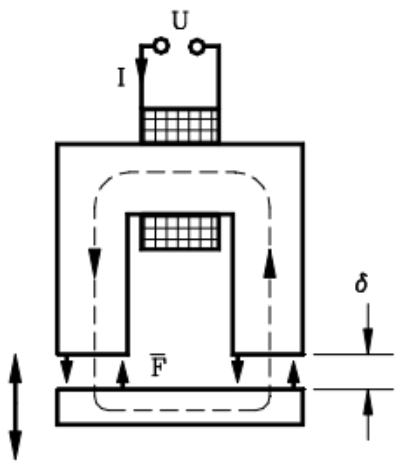


Fig.14 Magnetic circuit in an electromagnet[32]

For a simple electromagnet with a coil fed in direct current when passing through the excitation coil of current I, attractive forces appear on the separation surfaces of the fixed and movable armature that tend to reduce the δ .

The attractive force of a DC electromagnet[32] is determined from the magnetic energy Wm located throughout the system:

$$F = -\frac{\partial W_m}{\partial x}$$

The magnetic energy accumulated in a system can be defined by one of the following relationships:

$$W_m = \sum \frac{I_k \Phi_k}{2}$$

$$W_m = \int \frac{\overrightarrow{B} \cdot \overrightarrow{H}}{2} dV$$

Magnetic energy can be expressed in the form of

$$W = W_{\delta} + W_d + W_{miez}$$

where the first term defines the magnetic energy in the interfier, the second the dispersion energy and the energy contained in the stake of the magnet.

According to the energy balance of the electromagnet, the electromagnetic force exerted on the mobile system depends on the variation of the magnetic energy stored in the entire space occupied by the electromagnetic field of the electromagnet.

This space comprises the following distinct areas: working and parasitic interfiers, areas occupied by dispersion fluxes and ferromagnetic circuits.

In most cases, the magnetic voltage drop in the iron circuit is negligible and if iron saturation and field dispersion are neglected, it can be concluded that only the localized energy variation in the working irons will be taken into account when determining the attractive force.

For energy stored in the interfurnish:

$$W_d \cong \frac{BH}{2}A\delta = \frac{B^2}{2\mu_0}A\delta$$

For the magnetic circuit we can apply Kirchoff:

$$NI = H_{miez}L_{miez} + H_{intrefier}L_{intrefier} = B\left(\frac{L_{miez}}{\mu} + \frac{\delta}{\mu_0}\right)$$

In the design of electromagnets, material with high permeability is used (so the first term in the equation above is negligible compared to the second. Consequently: $\mu_r = 2000 - 6000$)

$$B \cong \frac{\mu_0 NI}{\delta}$$

Introducing into the energy formula we get:

$$W_d = \frac{\mu_0 N^2 I^2}{2\delta} A$$

Deriving we obtain the value of the force F developed by the electromagnet:

$$\mathbf{F} \cong -\frac{\partial}{\partial \delta} \left(\frac{\mu_0 N^2 I^2}{2\delta} A \right) = \frac{\mu_0 N^2 I^2}{2\delta^2} A = \frac{\phi^2}{2\mu_0 A};$$

N- number of turns of the coil; A- cross-section of the interfier; μ 0- magnetic permeability of vacuum and magnetic flux through interiron. Φ

Unlike DC electromagnets where the force is constant, AC electromagnets vary the flow over time so that the force has a pulsating variation.

If a sinusoidal variation in magnetic induction is allowed, the electromagnetic force has the expression:

$$F = -\frac{\Phi^2}{2\mu_0 A} = -\frac{\Phi_m^2}{2\mu_0 A} \sin^2(\omega t)$$

In the assembly in Fig.15 and Fig.16 is presented a device designed for the therapy of the lower limb and respectively an electromagnet from the system.

On the figure the notations are as follows: (1) Electromagnets; (2) plates that interact with the field generated by the electromagnet, closing the magnetic circuit, (3) copper coils, (4) high-permeability magnetic core that guides the magnetic field along it

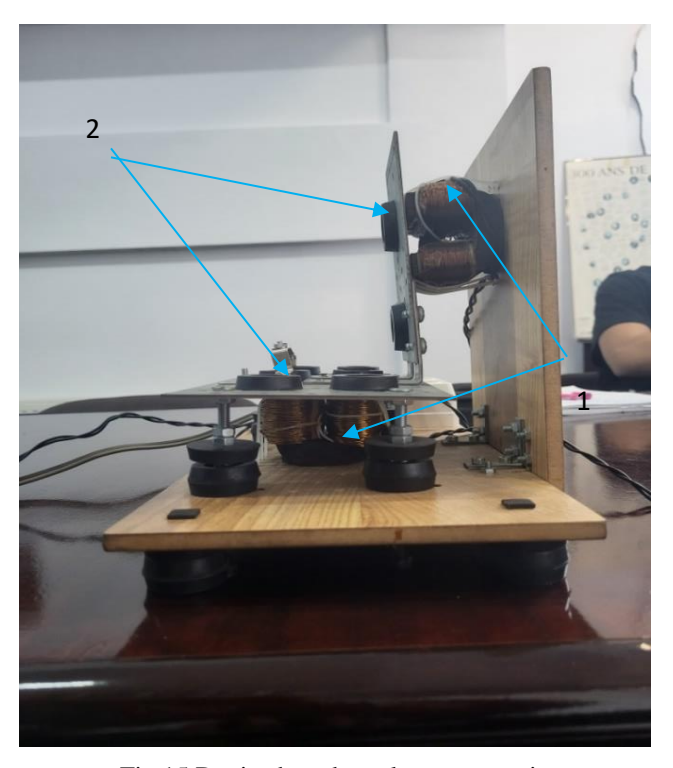


Fig.15 Device based on electromagnetic actuations



Fig.16 An electromagnet viewed on a larger scale

The coils are powered to an AC power source, thus creating a variable magnetic field. Due to the variable magnetic field, a variable electromagnetic force arises that drives the metal plates in an oscillatory motion. The vibration frequency of the plates is double the frequency of the supply current and can be adjusted to achieve different regimens depending on the patient's medical problems.

Although this device is not suitable to use in a hybrid actuator, it gives an understanding of how this type of actuators work.

The institute has previously manufactured a more compact electromagnetic actuator consisting of a coil with inductance of 38mH, resistance of 15.4Ω and 1325 turns. This actuator operates in the range of 12-24V, with an average displacement of 0.15mm/V.

4.5 Magnetostrictive actuators

Magnetostriction[34] is the property of some ferromagnetic materials to deform when magnetized. The effect was discovered by James Joule in 1842 while observing a nickel sample. The phenomenon is explained due to the fact that in the internal structure of a ferromagnetic material several domains can be distinguished, each of which represents a region with uniform magnetization. When a magnetic field is applied, the boundaries of these domains change shape, and the dipoles of each domain rotate (trying to align with the field). The reason why changes occur in the magnetic domains of the material leading to a deformation of the material itself is crystal anisotropy – the energy required to magnetize the crystal on one axis is less than on other axes.

If a magnetic field is applied at a certain angle to the "simplest" direction to magnetize the crystal, it will rearrange its domains so that the total energy of the system is the minimum possible.

Within magnetostriction, several important effects can be distinguished:

- The Joule effect occurs when material placed in a magnetic field undergoes elongation or compression
- Villari effect (inverse Joule) in a sample subjected to mechanical stress, a magnetic field proportional to the applied voltage is generated
- Wiedemann effect similar to the joule effect, when a magnetic field is applied, the material twists and deforms tangentially
- Matteuci effect (inverse Wiedemann) when the material is twisted, an inner magnetic field occurs.

The linearized constituent equations for one-dimensional models[33, 34], according to IEEE Standard 1991, have the expressions:

$$\varepsilon = S^H \sigma + dH$$
$$B = d^* \sigma + \mu^T H$$

Where -specific mechanical elongation, -unit mechanical effort, B-magnetic induction and H magnetic field intensity $\varepsilon\sigma$. S^H is elastic compliance in constant field; is magnetic permeability to constant mechanical tension and d and are magnetomechanical coefficients that can be determined experimentally using the relations: $\mu^T d^*$

$$d = \frac{\partial \varepsilon}{\partial H}\Big|_{T=ct}$$
$$d^* = \frac{\partial \varepsilon}{\partial H}\Big|_{H=ct}$$

The above equations can also be expressed as a function of relative deflection:

$$\sigma = E^H \varepsilon - eH$$
$$B = e^* \sigma - \mu^S H$$

Where is Young's modulus in $E^H=1/S^H$ constant magnetic field—note that Young's modulus is not constant, it exhibits a linear dependence on the applied field; is constant mechanical deformation permeability; again $\mu^S=\mu^T-dd^*/S^He=E^Hd; e^*=E^Hd^*$ The coupling coefficient of the material shall be defined:

$$k = \frac{\varepsilon_{mM}}{\sqrt{\varepsilon_m \varepsilon_M}};$$

Where it represents mechanical energy of elastic type, is magnetic energy and . We enter these expressions into the equation of k we get: $\varepsilon_m = \frac{S^H \sigma^2}{2} \; \varepsilon_M = \frac{\mu^T H^2}{2} \varepsilon_{mM} = \frac{dH\sigma}{2}$ $k = \frac{d}{\sqrt{\mu^T S^H}}$



Fig.17 Appearance of segments of a Terphenol-D bar

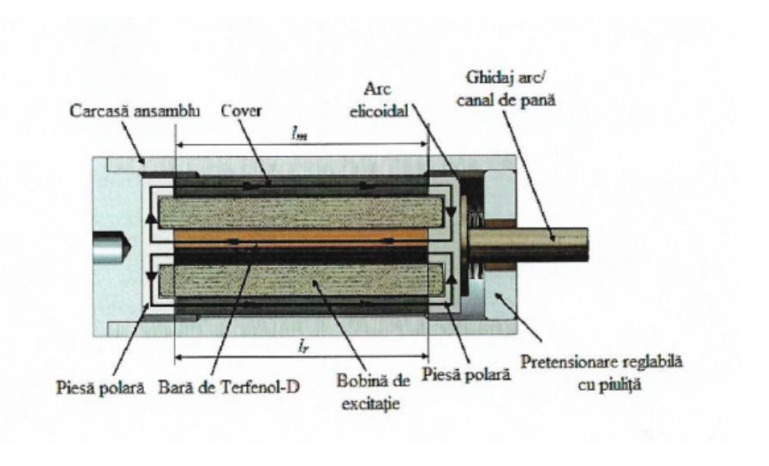


Fig.18 Diagram of a standard magnetostrictive actuator

One of the most widely used materials exhibiting strong magnetostriction in relatively low fields is the alloy Terphenol-D[34,36] (Ter-Terbium, Fe-iron, Nol-Naval Ordonance Laboratory, D-Dyprosium). It exhibits a positive magnetostriction (elongates in the presence of an external magnetic field) with values of order in magnetic fields. The Curie temperature for Terphenol-D is 650K and the saturation strain is about 2000ppm. A disadvantage of this material is its friability when stretching, having $\lambda = \frac{\Delta L}{L} = 1000 \div 2000 \ ppm50 \div 200 \ kA/m$ an allowable tensile stress between 28-40MPa (compared to compression which takes values between 305-880MPa).

Fig.18 shows the standard configuration of a magnetostrictive actuator. The actuator uses a cylindrical symmetry coil to apply a magnetic field to the Terphenol-D bar at the center of the actuator. At the end of

the actuator there are springs with a role in prestressing the material. Around the actuator or at its end are usually placed magnets that premagnetize the bar.

The premagnetization of the material fixes the operating point in the area where the slope of the specific deflection characteristic as a function of magnetic field H is maximum (blue area marked on Fig.19). This ensures the most efficient response of the actuator following the application of an external magnetic field $\lambda = \Delta L/LH_{ext}$

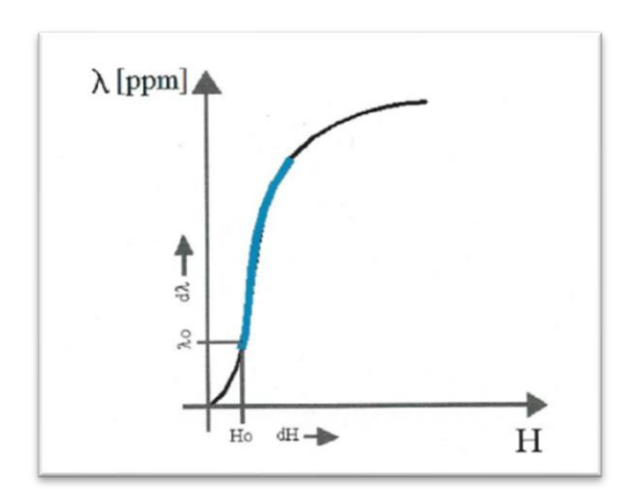


Fig.19 Specific deformation-magnetic field dependence for a Terphenol-D bar

Pretensioning is performed using springs that compress the bar, ensuring maximization of the bar's response to a certain applied field. There is an optimal pretension value for which the greatest deformation is achieved (in most cases about 2-3 times higher than in the absence of pretension). For values that are too high, the bar preformation decreases.

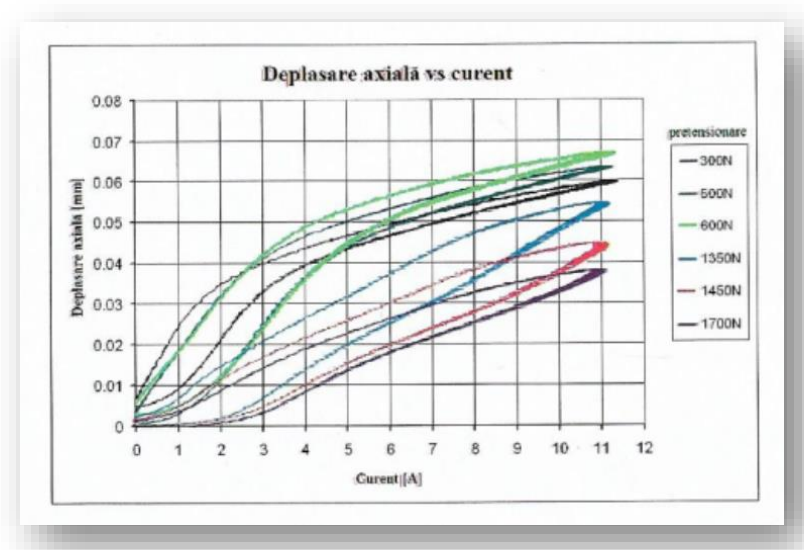


Fig.20 Hysteresis curves of the actuator for various pretensions

In the development of magnetostrictive force actuators there are two important impediments:

- Creating the necessary magnetic field by conventional methods (e.g. by using a coil) often leads to very high energy consumption. Also, due to the continuous passage of current through the coil, a cooling system and a system are required to compensate for the thermal expansion of the material caused by high temperatures.
- For actuators used for precise positioning, it is necessary that the power supply is very stable: the ratio between the amplitude of current fluctuations and the value of the current flowed by the source must be of any time. 10^{-7}

Several literature articles highlight the possibility of constructing magnetostrictive actuators for precise positioning using materials with smaller thicknesses, although in the vast majority of applications magnetostrictive actuators are used for the large forces and displacements they generate.

Magnetostrictive force positioner (MFP-1) and Magnetostrictive nanoscrew (MN-1) are actuators that do not have these impediments and have been developed and tested in Russia[36]. The main idea on which their solution is based is that these actuators only need to be powered during deformation and do not consume energy at all when stationary (they can memorize the position of the moving part of the actuator). These actuators can be controlled both manually and via a computer controlling multiple piezomotors. Manual control is done in increments of 3nm and via computer of 0.01nm. These types of actuators can be used in the manufacture of integrated circuits, in the manufacture of diffraction networks, control of a laser beam used in treatment centers, sensitive mass displacement of an electron microscope, etc.

5. Hybrid actuators

Following the measurements made and information extracted from the literature, it was concluded that the following hybrid actuators could be implemented:

- electromagnetic actuator combined with a piezoelectric actuator (PZT or collagen membrane)
- PZT actuator combined with an elastomer

These hybrid actuators have two modes of operation:

- ✓ rough mode performing large displacements (rough positioning step), and
- ✓ fine mode performing small movements (precise positioning stage).

In this way, the above actuators can provide positioning with increased precision for different ranges.

5.1 Test of hybrid electromagnetic - piezoelectric actuator

The actuator in Fig.21 was built in order to test and measure various parameters related to the performance of the hybrid electromagnetic - piezoelectric actuator.

The actuator labeled with number 1 represents the electromagnetic actuator, which moves strictly on the vertical axis of the image (Oz axis). Actuators labeled with number 2 are PZT piezoelectric actuators, each controlling one axis.

Measurements were made on each independent element and the data was listed in the tables below

Table 6. Measurements performed on the electromagnetic actuator

F[cN]	d[<i>mm</i>]	U[V]	I[A]
21	10,16	5	1,91
28	12,15	10	2,8
31	16,18	20	3
33	21,10	30	3,2

Table 7. Measurements performed on the piezoelectric actuator

U[V]	$d[\mu m]$	F[mN]
1	0,05	3
3	1	5
5	2,1	5,8
8	3,4	6,3
10	4,7	7,5

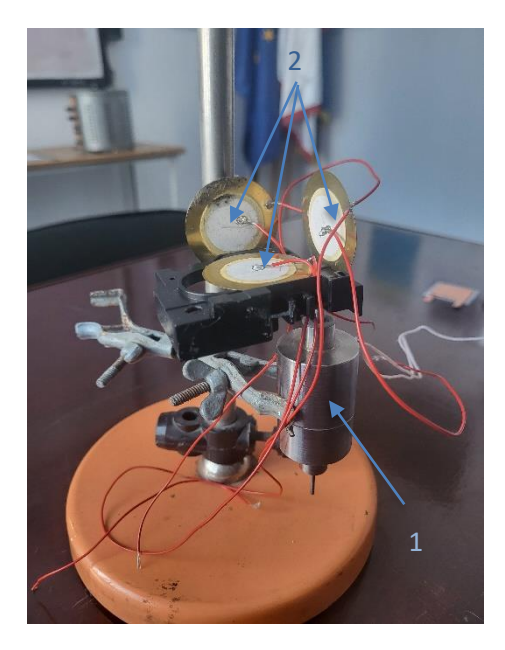


Fig.21 Appearance of the electromagneticpiezoelectric actuator

The voltage displacement dependencies for each actuator were plotted:

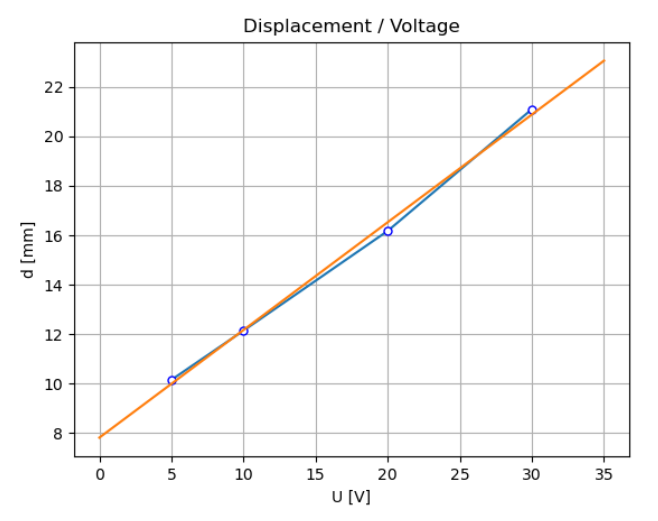


Fig.22 Displacement-voltage characteristic for electromagnetic actuator. The orange line linearly fits the points joined by the blue line.

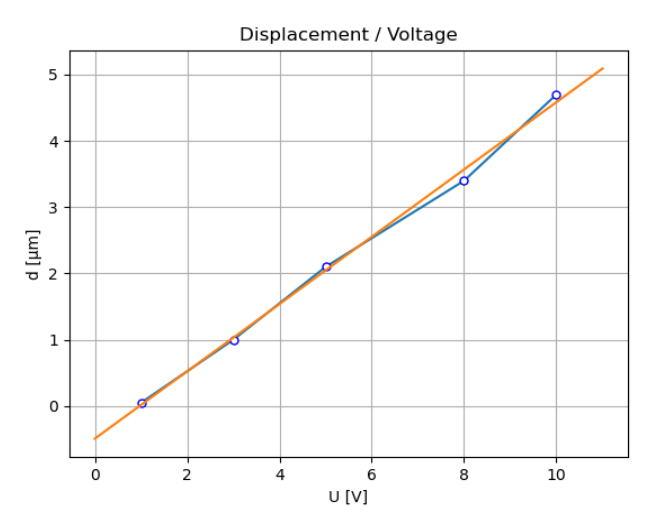


Fig.23 Displacement-voltage characteristic for piezoelectric actuator. The orange line linearly fits the points joined by the blue line.

For the electromagnetic actuator the slope of the graph is 0.4354 mm / v, the intercept at the origin is 7.822 mm. For piezoelectric the slope of the characteristic is 0.5075 μ m/V, and the intercept at origin is 4.906 μ m. The initial deformation of the piezoelectric actuator is replicated by the fact that the retroreflector of the interferometer, which has been placed on the actuator, exerts pressure on it, thus compressing it. In the case of the electromagnetic actuator, the initial deformation is due to the way the digital indicator (with which the measurements were taken) was coupled to the actuator.

Regarding the technical parameters of the system, for the electromagnetic actuator a source that can flow up to 50V offers the possibility of executing displacements up to 21.75mm, which is a fairly wide range for the rough positioning stage. Considering that we use the piezoelectric actuator for displacements below 0.02mm (for larger displacements the electromagnetic one can be used), this would mean that a source that can flow up to 50V is required to ensure this deformation range. These voltage domains are large but not particularly required; they represent only an upper limit. This actuator fulfils its intended purpose, namely precise positioning with micron precision. This actuator could be used in optical systems that require very precise alignment to achieve the best results (e.g. interferometry).

5.2 PZT-elastomeric hybrid actuator

To make the elastomeric membrane actuator more efficient, the substance of which the elastomer is composed was mixed with pyrite. Thus, by injecting particles of conductive material, it deforms more easily at lower voltages. This is advantageous because the actuator consumes less and there is no need to use a high voltage source.

In Fig.24 we can see the structure of this hybrid actuator:

- 1- Lower electrode of PZT disc actuator
- 2- PZT piezoelectric material disc
- 3- Middle electrode (lower for elastomer actuatotor)
- 4- Elastomeric membrane
- 5- Upper electrode of elastomeric actuator

In order to discuss the performance of this actuator, each element was analysed separately, the results being listed in Table 8 for the PZT disc and Table 9 for the elastomeric membrane.

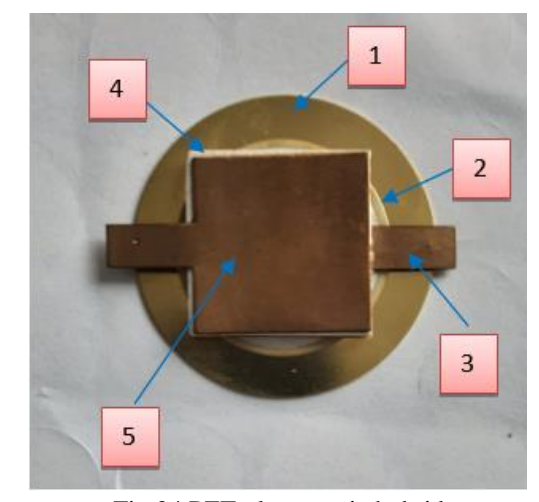


Fig.24 PZT-elastomeric hybrid actuator

Table 8. Measurements on the PZT actuator

U[V]	$d[\mu m]$	F[mN]
3.7	2	2.8
5	2.6	6
8	3.7	7.1
10	4.7	7.5

Table 9. Measurements on elastomeric actuator

U[V]	$d[\mu m]$	F[mN]
60	0,4	1,8
80	0,9	2,2
100	1,6	3
110	1,9	4,2

Proceeding as with the hybrid electromagnetic - piezoelectric actuator, plot the voltage displacement dependencies for each actuator:

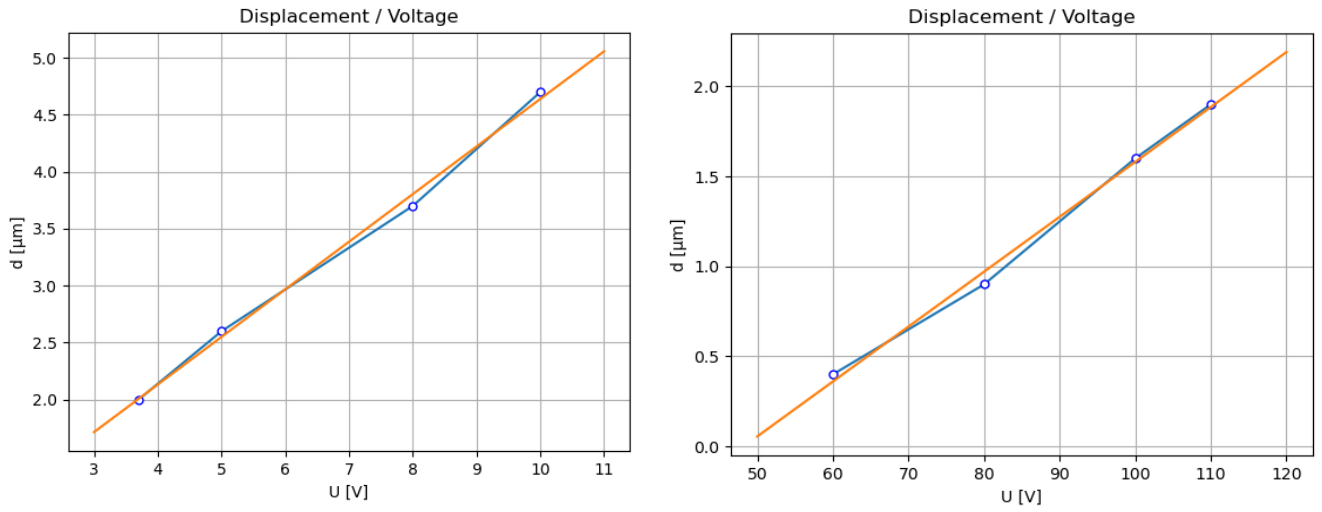


Fig.25 Displacement-voltage characteristic for PZT actuator. The orange line linearly fits the points joined by the blue line.

Fig.26 Displacement-voltage characteristic for elastomeric actuator. The orange line linearly fits the points joined by the blue line.

For the PZT actuator the slope of the graph is $0.418 \mu m/V$, the initial intercept is $0.4605 \mu m$. For the elastomeric membrane the characteristic slope is 30.5 nm/V, and the initial intercept is $-1.47 \mu m$. The initial deformation of both actuators is due to factors related to the measuring apparatus. In the case of the elastomeric actuator, the deflection arises from the weight of the retroreflector pressing on the element during measurement. For this reason, the intercept does not play an important role in our analysis, the significance of our measurements residing in the slope.

This actuator has the same principle of operation as the electromagnetic one - piezoelectric: in this case, the PZT one is used for the rough positioning stage, and the elastomeric membrane one for the precise positioning stage. Thus, the actuation range for relatively low voltages (<50V) extends to approximately 21 μ m with an accuracy of 1-10 nanometers (depending on the capabilities of the elastomeric actuator power supply).

6. Conclusions and Discussion

- Within this project, multiple measurements were performed that led to the characterization of many electromechanical actuators, starting from those that develop relatively small deformations and forces (PZT, polymer membranes, etc.) to those that perform large displacements (magnetostrictives, electromagnetics).
- Two hybrid actuators were built, both of which lived up to theoretically predicted performance. For the electromagnetic piezoelectric actuator, the operating regimes of each actuator have been established:

Electromagnet- 0.4354mm/V Piezoelectric PZT-0.5075μm/V

And respectively, for the PZT actuator - elastomeric:

PZT actuator-0.418μm/V Elastomeric membrane-30.5nm/V

The PZT disc can be used over a wide range of voltages and is also resistant to high voltages. The elastomeric membrane could also be used at higher voltages, but it is not necessary as larger displacements can be performed with the PZT actuator.

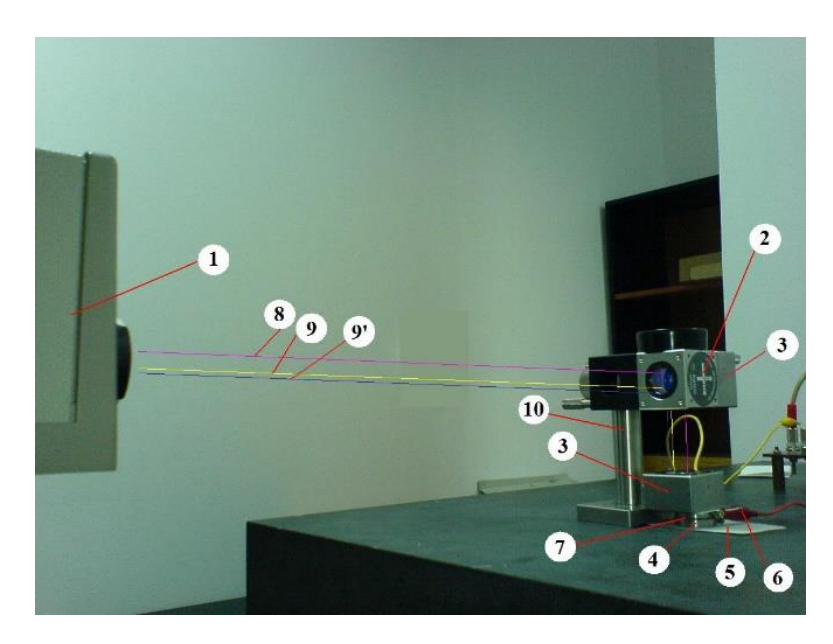
To increase the accuracy of the elastomer, a variant of the elastomer can be used that has not been doped with pyrite / other conductive materials, but this comes with the disadvantage that higher voltages are required to cover the entire range of displacements covered by the one used in the model above.

Both devices have possibilities of adaptation and miniaturization depending on the applications in which they are used.

- One of the areas where these actuators could be used is optics.
 - In most experiments/works using optical systems, component alignment is a very important factor that can significantly affect the quality of measurements.
 - Even more so in the case of interferometers and other wave optics experiments. Using the actuators mentioned above, precise alignment of system components could be achieved.
- It would also be interesting to implement an actuator that is composed of the 3 elements (electromagnetic PZT elastomer). It could have 3 positioning steps, starting from a few millimeters to a few nanometers.

Annex I - Apparatus used to measure small movements

All measurements performed on membranes in this article were made using an interferometer with nanometer precision shown in Fig.27.



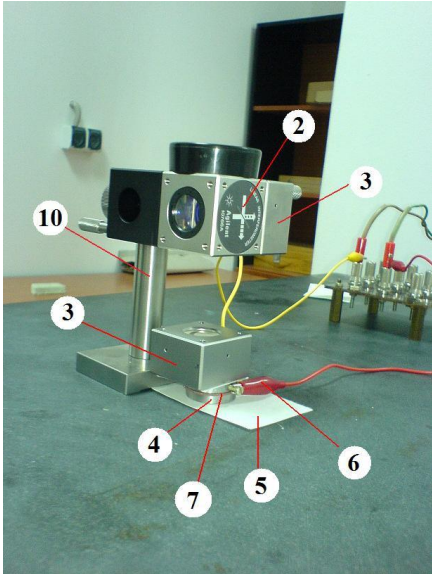


Fig.27 Michelson-type interferometer used to determine membrane deformations, made by Agilent.

The equipment for determining sample deformation (membrane, piezoelectric actuator) consists of:

- 1 laser head placed on an adjustable tripod;
- 2 linear interferometer with attached linear retroreflector;
- 3 two linear retroreflectors;
- 4 special power electrodes (in the case of piezoelectric motor they are attached directly from the construction);
- 5 insulating film;
- 6 power cord;
- 7 sample (membrane, ultrasonic motor) to measure;
- 8 laser beam generated by the laser head;
- 9 laser beam reflected back to the laser head detector, from the linear retroreflector attached to the interferometer;
- 9 laser beam reflected back from the linear retroreflector placed over the sample to be measured;
- 10- interferometer stand.

The optical interferometer is fixed to a stand and will be placed so that we achieve the best possible alignment of the reflected wave. In order to have as small measurement errors as possible, it is

recommended that the reflected wave be aligned in a proportion of more than 70%. The Agilent interferometer installation contains advanced software that also displays alignment accuracy.

In order to obtain a very precise alignment, the linear retroreflector placed over the sample to be measured will be moved each time together with the sample to be measured.

The electrodes and the measuring membrane cannot have very small dimensions compared to the dimensions of the reflector, because the mechanical stability of the sample-retroreflector assembly may be damaged and implicitly the entire measuring system will become unstable.

Since the membranes have a piezoelectric character, the weight of the retroreflector must also be taken into account, which compresses the material and gives it an initial deformation. Therefore, the axis on the graphs on which the membrane movement is represented must be aligned so that when voltage is not applied, the system indication is 0.

Annex II – Bibliography

- [1] C.Mocanu, "Theory of the electromagnetic field", Didactic and Pedagogical Publishing House, Bucharest, 1981
- [2] K. Simonyi, "Theoretical Electrotechnics", Technical Publishing House, Bucharest, 1974.
- [3] Edward Purcell, "Berkeley Physics Course. Electricity and Magnetism", Vol. II, Ed. Didactică și pedagogică, Bucharest, 1982.
- [4]U.H.Schaim, J.B.Cross, J.H.Dodge, J.A.Walter,"Physics: The Student's Text," Ed. Didactics and Pedagogics, Bucharest, 1984.
- [5] Ignat M., "Theoretical Aspects on Ponderomotive Forces"
- [6] Ignat M., "Piezoelectric micromotors and microactuators", Ed Electra, 2005.
- [7]Ignat M., Amza Gh., Haraguta Cr., "Unconventional electromechanical actuators", Electra Publishing House, 2003
- [8] Daniel Kuang-Chen Liu, James Friend, Leslie Yeo "A brief review of actuation at the micro-scale using electrostatics, electromagnetics and piezoelectric ultrasonics", Acoustical Science and Technology, 2010
- [9]Gassert R., Yamamoto A., Chapuis D., Dovat L., Bleuler H, Burdet E, "Actuation Methods for Applications in MR Environments", Concepts in Magnetic Resonance Part B-magnetic resonance Engineering, 2010
- [10] Mulukutla S. Sarma, "Introduction to Electrical Engineering", Oxford University Press, 2010
- [11] R. Voinea, D. Voiculescu, Fl.P.Simion, "Introduction to solid state mechanics, with applications in engineering", Ed.Academiei", 1989.
- [12] R. Feynman, "Modern Physics, Vol.I", Technical Publishing House, Bucharest, 1970.
- [13] V. I.Arnold,"Mathematical methods of classical mechanics", Scientific and Encyclopedic Publishing House, Bucharest, 1980.
- [14] Marcel N.Roșculeț "*Mathematical Analysis*", vol. I and II", Ed. Didactics and Pedagogics, Bucharest, 1967.
- [15] I.Gh.Şabac," Matematici speciale 2", Ed.Didactică și pedagogică Bucharest, 1965.
- [16] B. Tareev, "Physics of dielectric materials", MirPublishers Moscow, 1975

- [17]. V. V.Sîcev, "Complex thermodynamic systems", Scientific and Encyclopedic Publishing House, Bucharest, 1982.
- [18] E. Jantsch, "Technological forecast", Scientific Publishing House, Bucharest, 1972.
- [19] Ignat M., "Initiation in scientific research", Electra, Bucharest, 2017.
- [20] Ignat M., "How to choose a research theme", Electra, Bucharest, 2018
- [21] L.W.Crum, "Value Engineering", Ed. Tehnic, Bucharest, 1976.
- [22] Ignat M., G.Hristea, G.Telipan, "Electromechanical actuators and unconventional sensors", Electra Publishing House, Bucharest, 2004.
- [23] D. Bushko, I.Goldie, "High Performance Magnetostrictive Actuators", IEEE AESSystems Magazine, November, 1991, p21-25
- [24] M. Ignat, I.Puflea, G.Zărnescu, L.Pâslaru, Al.Cătănescu, V.Stoica, "Electromagnetic actuators", Electra Publishing House, Bucharest, 2008.
- [25] R.Hanitsch, "Microactuators and Micromotors", Proceedings of the Aegean Conference on Electrical Machines and Powered Electronics, Kusadasi, Turkei, 5-7 June 1995, vol. I, pp.119-128.
- [26] W.G.Cady, "Piezoelectricity.An introduction to the theory and application of electromechanical phenomena in crystals", Dover Publication, Inc, New York, 1964.
- [27] S. Ueha, Y.Tomikawa, M.Kurosawa, "Ultrasonic Motors.Theory and Applications", Clarendon Press Oxford, 1993.
- [28] R. Bansevicius, K.Ragulskis, "Vibromotors for precision microrobots, Hemisphere Publishing Corporation", New York, 1988.
- [29] M. Ignat, "Unconventional microelectromechanical 3D drive system with piezoelectric microactuators", 6th, International Symposium on Advanced Motion Systems, ELECTROMOTION 2005, Laussane, Switzerland, 27-29september 2005.
- [30] Th.Kuhn, The Structure of Scientific Revolutions, Scientific and Encyclopedic Publishing House, Bucharest, 1976.
- [31]Kenji Uchino, "Introduction to Piezoelectric Actuators and Transducers", International Center for Actuators and Transducers, Penn State University, PA 16802
- [32] http://mec.upt.ro/dolga/cap5.pdf
- [33] Alison B. Flatau, Marcelo J. Dapino and Frederick T. Calkins "On Magnetostrictive Transducer Applications", Materials for Smart Systems III, Materials Research Society Symposium Proceedings Volume 604
- [34] Cătănescu Alexandru-Laurențiu, scientific advisor: Prof. Dr. Ing. Caesar Fluerașu "**Referat nr. 1: Theoretical bases of magnetostriction phenomenon**", Faculty of Electrical Engineering, UPB, Department of Electrical Engineering
- [35] Cătănescu Alexandru-Laurențiu, scientific advisor: Prof. Dr. Ing. Caesar Fluerașu "**Referat nr. 2: Applications of magnetostrictive actuators in electrical drives**", Faculty of Electrical Engineering, UPB, Department of Electrical Engineering
- [36] S.E. Tsodikov, V.I. Rakhovsky "Magnetostrictive Force Actuators for Superprecise Positioning", AV Technology Ltd., Moscow, Russia

【評語】100049

- 1. The report reviewed many type of actuators. Authors should make it more clear about what types of actuators are studied herein and elaborate the specifications of these actuators.
- 2. Authors are advised to analyze the performance (such as, but not limit to response time) thoroughly.
- 3. In addition to describing the engineering process of this research work, it would be good (also required) to present the innovation of this work. A comparison of the proposed system with existing state-of-the-art methods should be provided in the introduction so the advances, contributions, and novelty of the approach can be identified.
- 4. It would be good to include a design philosophy to let the reader understand the methodology of this design. In addition, an experimental evaluation that combines both macro and micro-movements is suggested
- 5. The figure on page 10 was labeled "Fig 3". It is unclear where is figure 1 and 2 since the figure on page 4 was not labeled.
- 6. On page 11, please provide a detailed explanation of the differences between membrane PE2, PE3, and PE4.

7. The authors are strongly advised to provide a comprehensive description of the device's fabrication process and the methodology employed to obtain the obtained results.